Measurement of F_2 and R on Nuclear Targets in the Nucleon Resonance Region

Vahe Mamyan

April 28 2009

Physics Motivation

- ✔ Quark-hadron duality to investigate the transition from the perturbative to the non perturbative region of QCD.
- ✔ Understand the nuclear dependence of R and it's relation to nuclear physics.
- ✔ Separation of vector and axial-vector components in neutrino scattering is only possible if the vector part is provided from electron scattering experiments.
- ✔ Experiments like MINERvA, MiniBONNE, K2K intend to study neutrino oscillations. Nuclear structure functions will be used as input data for these experiments.
- ✔ Measurements of SF in the resonance region may allow to determine SF in the high x region which is kinematically inaccessible.

QCD and the Strong Force

- ✓ **QCD is the theory of strong interactions. Two of its most important properties are:**
  - ➢ **Asymptotic freedom, quarks are considered free at small distances.**
  - ➢ **Quark confinement, no free quark was discovered.**
- ✓ **No phase transition from confinement to asymptotic freedom.**
- ✓ **The phenomenon of quark-hadron duality can help to investigate the nature of the transition from the perturbative (asymptotic freedom) to the non perturbative (quark confinement) region of QCD.**

Quark-Hadron Duality

Bloom and Gilman: the average over resonances produced in eN scattering closely resembles the scaling function measured in the deep inelastic region.

- ✓ **Explaining observed duality in the basis of QCD is a major step in understanding the nuclear force.**
- ✓ **Moments of the Structure Functions.**

$$M_2^{(n)}(Q^2) = \int_0^1 dx\, x^{n-2} F_2(x, Q^2)$$

$$M_2^{(n)} = \sum_{\tau=2,4,..}^{\infty} \frac{A_\tau^{(n)}(\alpha_s(Q^2))}{Q^{\tau-2}}$$

- ✔ **Theoretical basis for duality is OPE.**
- ✔ **Duality can happen if higher twist contributions are small or cancel.**

E.D. Bloom and F.J. Gilman
Phys. Rev. Lett. 25, 1140 (1970)

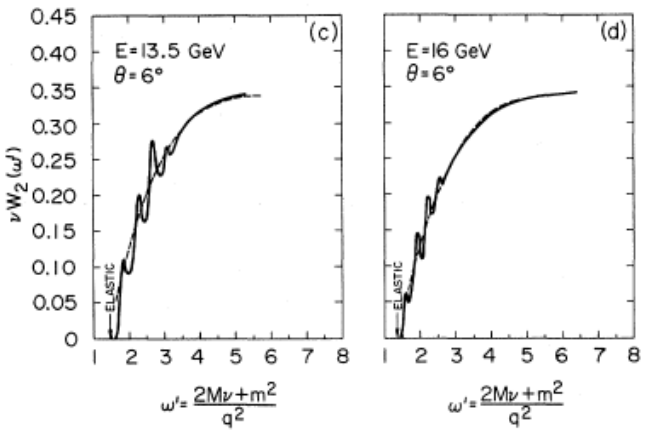

The Nuclear Dependence of R

Left-World's data of R at high Q^2 in the DIS region for nucleons and nuclei.

Right- SLAC E140 data, nuclear dependence of (R_A-R_D) in DIS.

$$R = \frac{\sigma_L}{\sigma_T} = \frac{F_L}{2xF_1}$$

Picture from E04-001 proposal

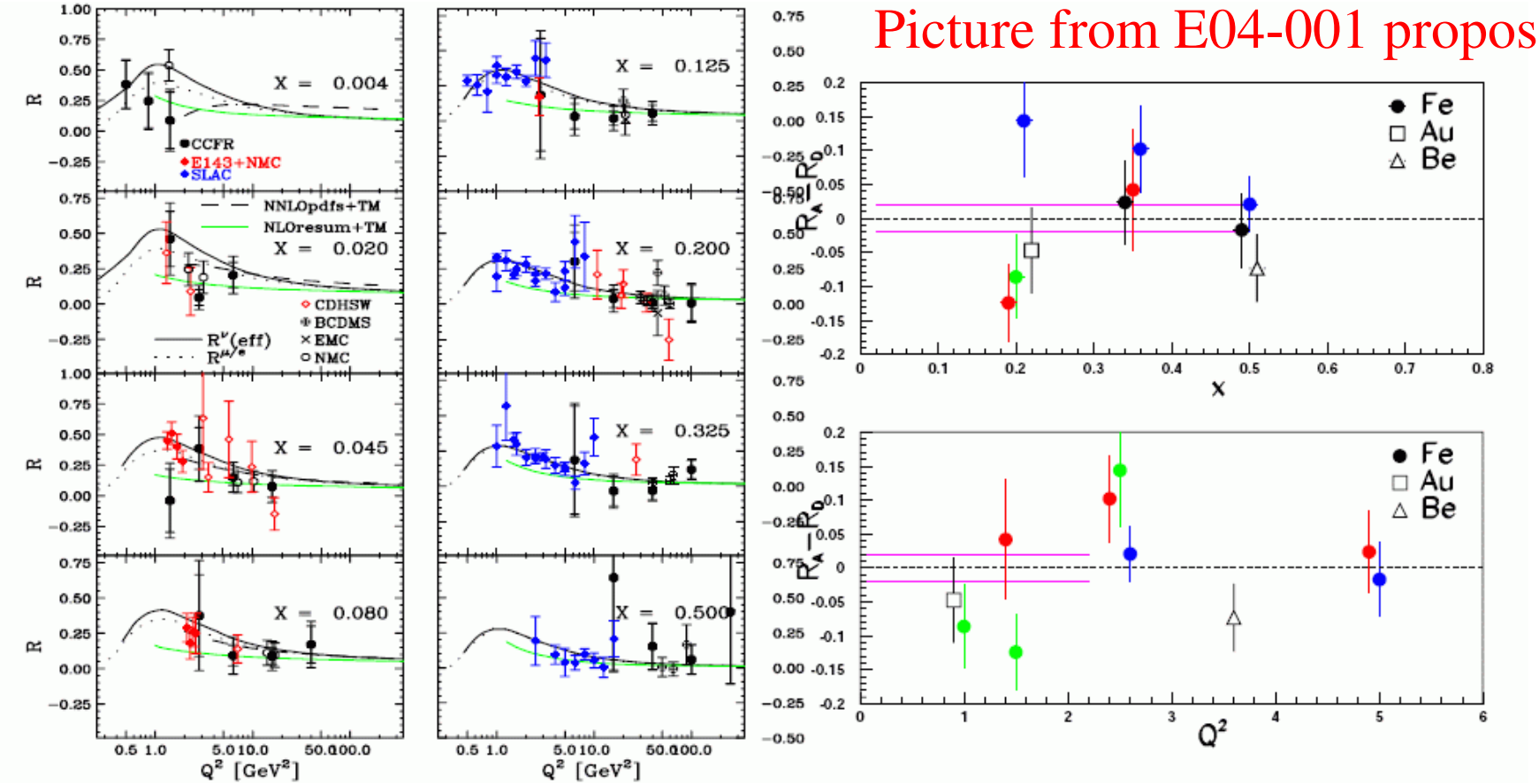

A comparison of the ratio of cross section of iron to deuterium in the resonance region versus in the DIS region. This data support that there are no nuclear dependence of R.

$$\xi = \frac{2x}{1+\sqrt{1+4M^2x^2/Q^2}}$$ **Nachtmann scaling variable**

Picture from E04-001 proposal

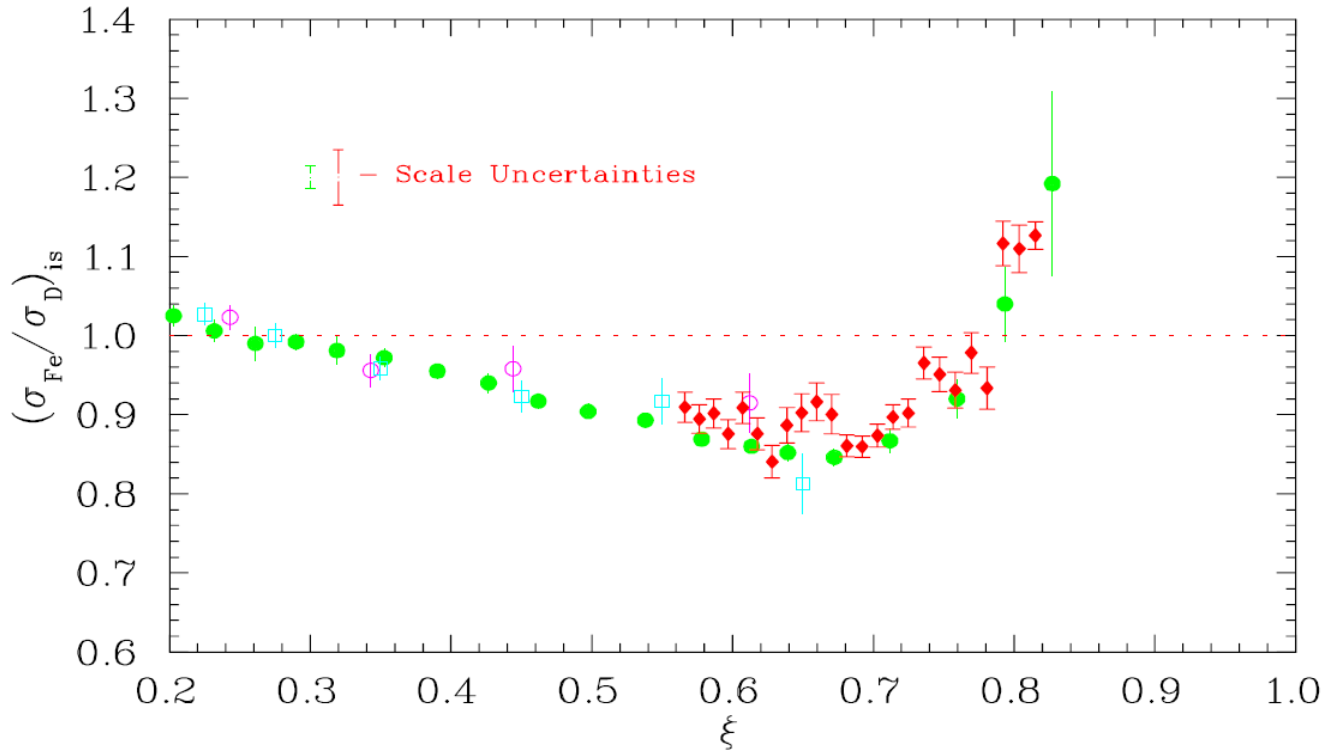

The Nuclear Dependence of R

Plot from G.A. Miller(Phys.Rev. C64, 022201)

The measurement of R in the kinematic region of this experiment provides information about the dynamics of nuclear force inside nuclei.

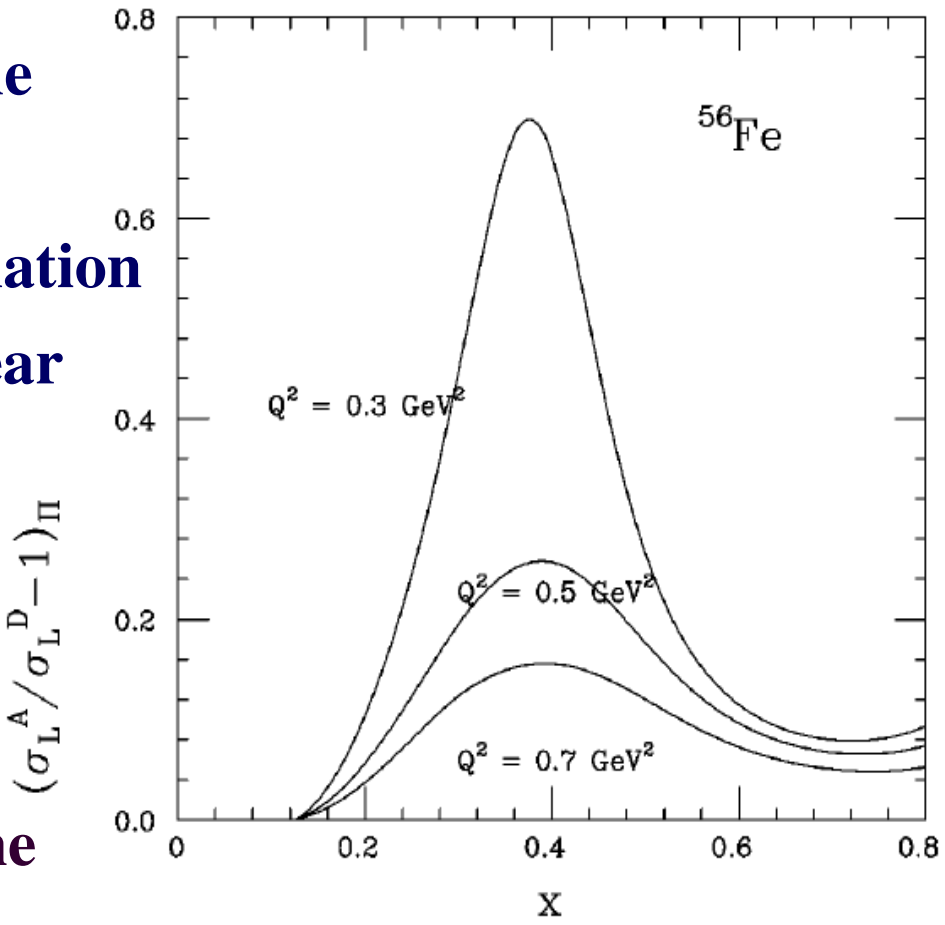

Study of A dependence of the longitudinal cross section.

Inelastic Electron Scattering

One photon exchange approximation.

$$\frac{d^2\sigma}{d\Omega\, dE'} = \frac{\alpha^2}{Q^4}\frac{E'}{E} L_{\mu\nu} W^{\mu\nu}$$

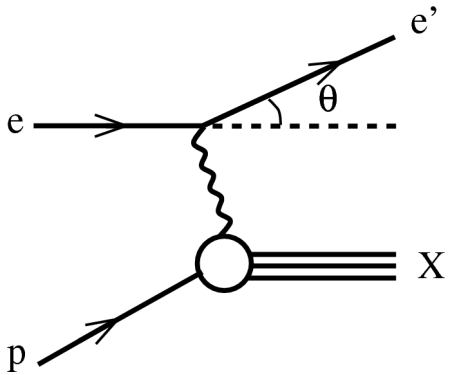

If the initial proton is not polarized the general form of hadron tensor can be written as

$$W^{\mu\nu} = W_1 g^{\mu\nu} + \frac{W_2}{M^2} p^\mu p^\nu + \frac{W_4}{M^2} q^\mu q^\nu + \frac{W_5}{M^2}(p^\mu p^\nu + q^\mu q^\nu)$$

Since the $L_{\mu\nu}$ is symmetric in $\mu\nu$ and $q_{\mu\nu}W^{\mu\nu} = 0$ (gauge invariance) there are only two independent structure functions, W_1 and W_2.

$$\frac{d^2\sigma}{d\Omega\, dE'} = \frac{4\alpha^2 (E')^2}{Q^4}\left[\cos^2\frac{\theta}{2} W_2(\nu, q^2) + 2W_1(\nu, q^2)\sin^2\frac{\theta}{2}\right]$$

The two structure functions are related to photo-absorbtion cross section for transverse photons and longitudinal photons.

$$W_1 = \frac{K}{4\pi^2\alpha}\sigma_T \qquad \textbf{where} \qquad \sigma_T = \frac{1}{2}\left(\sigma_+ + \sigma_-\right) \qquad K = \frac{2M_P\nu - Q^2}{2M_P}$$

$$W_2 = \frac{K}{4\pi^2\alpha}\left(\sigma_T + \sigma_L\right)\frac{Q^2}{Q^2+\nu^2}$$

$$\frac{d^2\sigma}{d\Omega\, dE'} = \Gamma\left(\sigma_T + \epsilon\,\sigma_L\right) \qquad \Gamma = \frac{\alpha E'\left(W^2 - M_P^2\right)}{2\pi Q^2 M_P E(1-\epsilon)} \qquad \epsilon = \left[1 + 2\left(1 + \frac{\nu^2}{Q^2}\right)\tan^2\frac{\theta}{2}\right]$$

$$\frac{d^2\sigma}{d\Omega\, dE'} = \Gamma\,\frac{4\pi^2\alpha}{x\left(W^2 - M_p^2\right)}\left[2xF_1\left(x, Q^2\right) + \epsilon\left(\left(1 + \frac{4M_P^2x^2}{Q^2}\right)F_2\left(x, Q^2\right) - 2xF_1\left(x, Q^2\right)\right)\right]$$

$F_1\left(x, Q^2\right)$ **is purely transverse,**

$$F_L = \left(1 + \frac{4M_P^2x^2}{Q^2}\right)F_2 - 2xF_1 \qquad \textbf{is longitudinal} \qquad R = \frac{\sigma_L}{\sigma_T} = \frac{F_L}{2xF_1}$$

Neutrino Structure Functions

In neutrino scattering, analogy to electron scattering, W absorption cross section for left, right handed and scalar is $\sigma_L, \sigma_R, \sigma_S$.

$$W_1 = \frac{K}{\pi G\sqrt{2}}\left(\sigma_R + \sigma_L\right) \quad W_2 = \frac{K}{\pi G\sqrt{2}}\frac{Q^2}{Q^2+\nu^2}\left(\sigma_R + \sigma_L + 2\sigma_S\right) \quad W_3 = \frac{K}{\pi G\sqrt{2}}\frac{2\mathrm{M}}{\sqrt{Q^2+\nu^2}}\left(\sigma_R - \sigma_L\right)$$

One important difference from EM case is that $W_{1,2}$ contain both VV and AA terms. W_3 is a result of V-A interference.

Conservation of vector current in EM processes allows to relate structure function to it's counterparts in neutrino scattering for specific isospin final states.

- ✔ **Electromagnetic scattering probes the charge of the partons.**
- ✔ **Neutrino scattering probes the flavor composition of the partons (charge conservation at the quark vertex).**

Relation of Structure Functions in QPM

$$F_2^l(x) = \sum_i e_i^2 \, x f_i(x)$$

Electromagnetic structure function.

$$F_2^\nu(x) = 2\sum_i \left[x q_i^\nu(x) + x \bar{q}_i^\nu(x) \right]$$

Neutrino structure function.

$$\frac{F_2^{lN}}{F_2^{\nu N}} = \frac{5}{18}\left(1 - \frac{3}{5}\frac{x s + x \bar{s} - xc - x \bar{c}}{x q + x \bar{q}}\right)$$

This relationship is known as 5/18 ths rule.

The relation of charged lepton scattering structure function to neutrino scattering structure functions is an important achievement of Quark Parton Model.

This relation was confirmed experimentally!

Rosenbluth Separation Technique

$$\frac{d^2\sigma}{d\Omega\, dE'} = \Gamma\left(\sigma_T + \epsilon\,\sigma_L\right)$$

Γ **Flux of transverse virtual photons.**

ϵ **Relative flux of longitudinally polarized virtual photons.**

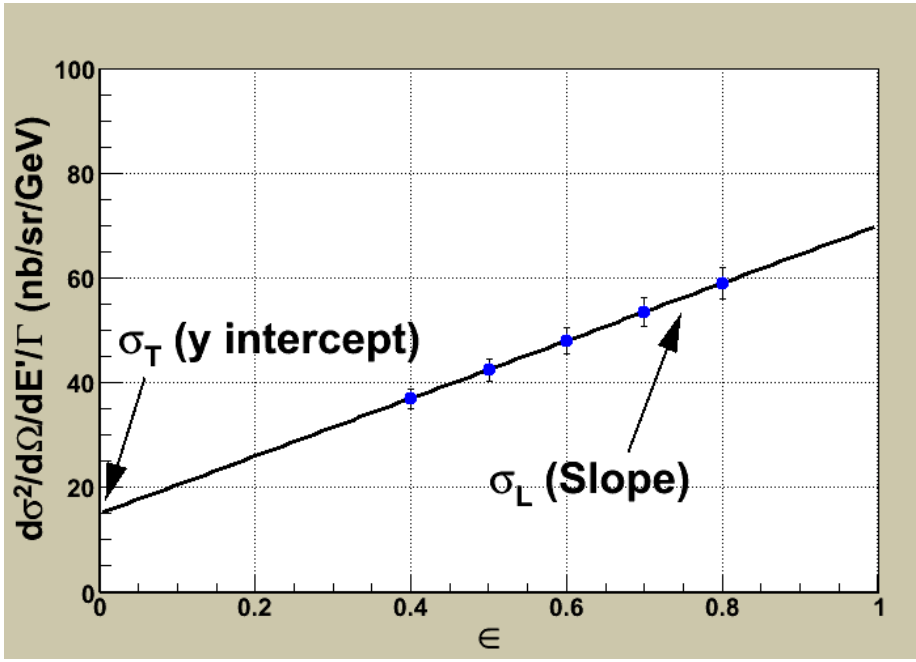

$$R = \frac{\sigma_L}{\sigma_T} = \frac{F_L}{2xF_1}$$

Rosenbluth separation can be done by making measurements at two or more values of ε for fixed W^2 and Q^2.

Experimental Hall C

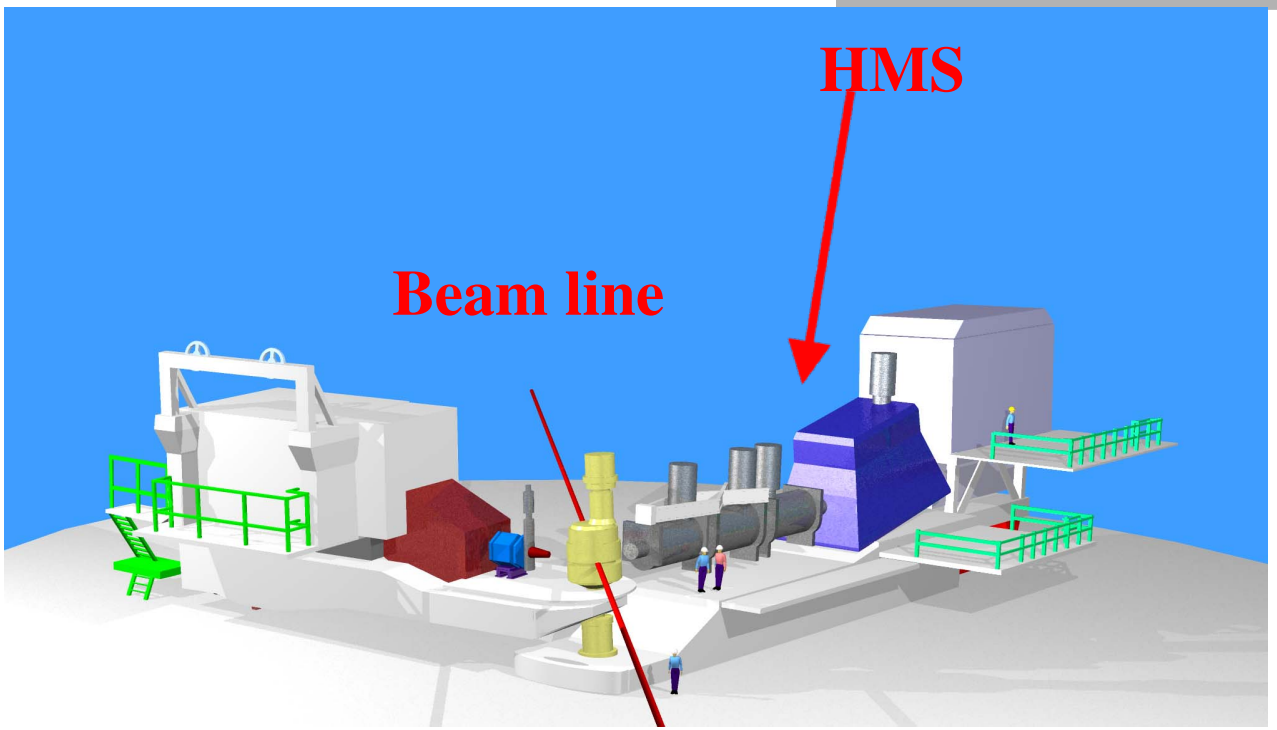

Electron beam energy – 0.7 – 5.7 GeV

HMS – High Momentum Spectrometer

- ✓ **Maximum central momentum – 7.5 GeV/c**
- ✓ **Momentum bite – 15 %**
- ✓ **Solid angle – 6 msr**
- ✓ **Luminosity $> 10^{38}$ cm^{-2} sec^{-1}**

Experimental Setup

$$e + A \rightarrow e' + X$$

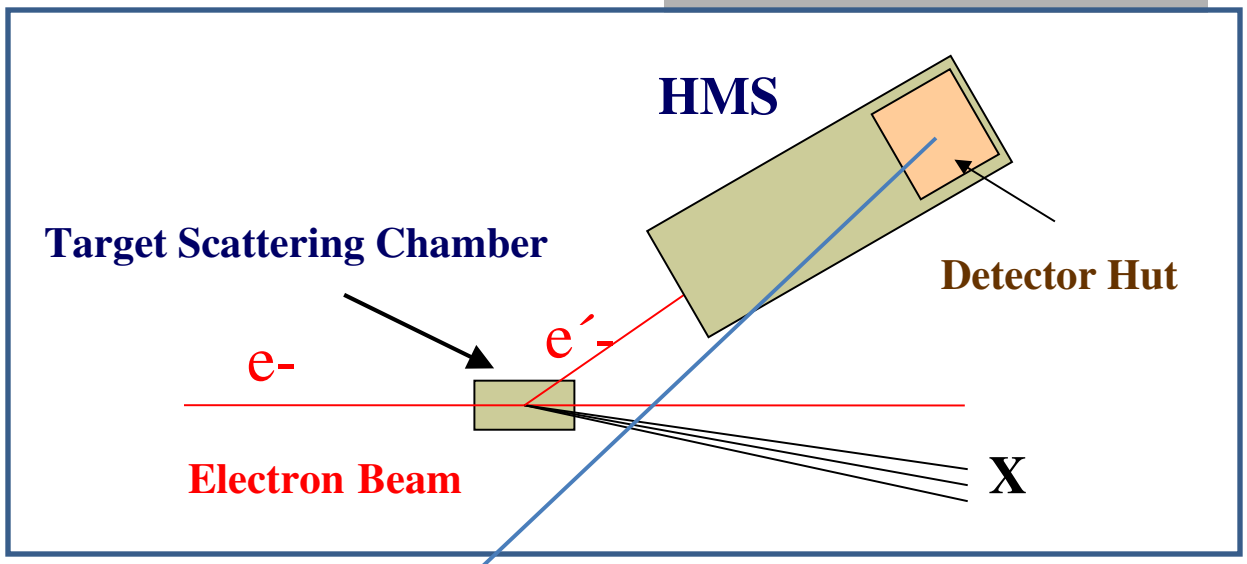

Drift Chambers,
Horizontal and vertical

Gas Cerenkov

Calorimeter

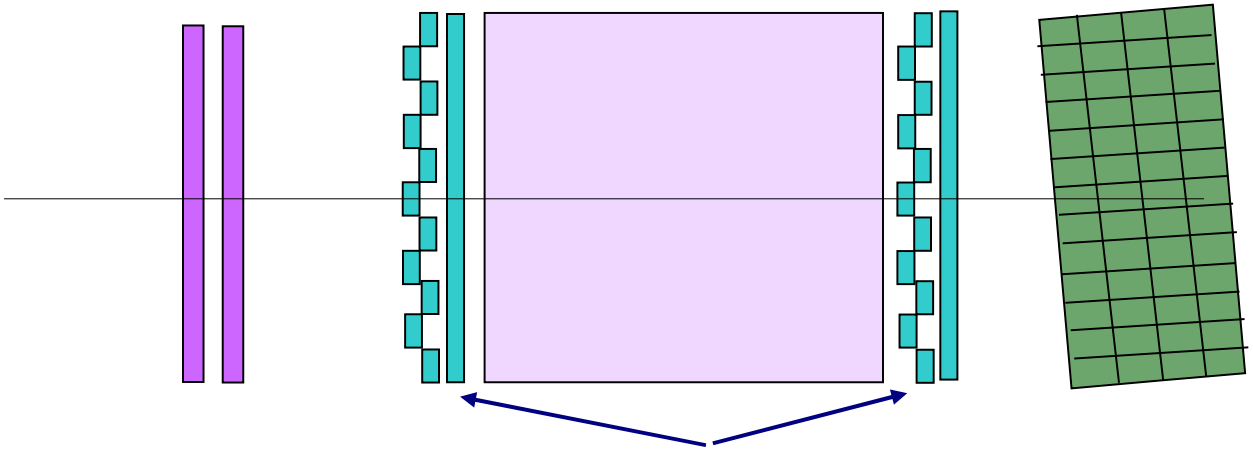

Vertically and Horizontally segmented hodoscopes

Gas Cerenkov and calorimeter provide pion rejection of 10000:1 at 1 GeV

Drift Chambers

Two drift chambers to measure particle coordinates and momentum.

Each drift chamber has six planes to measure particle angles. Covers 113x52 cm^2.

Sense wires are 1 cm apart, gas is a mixture of argon and ethane.

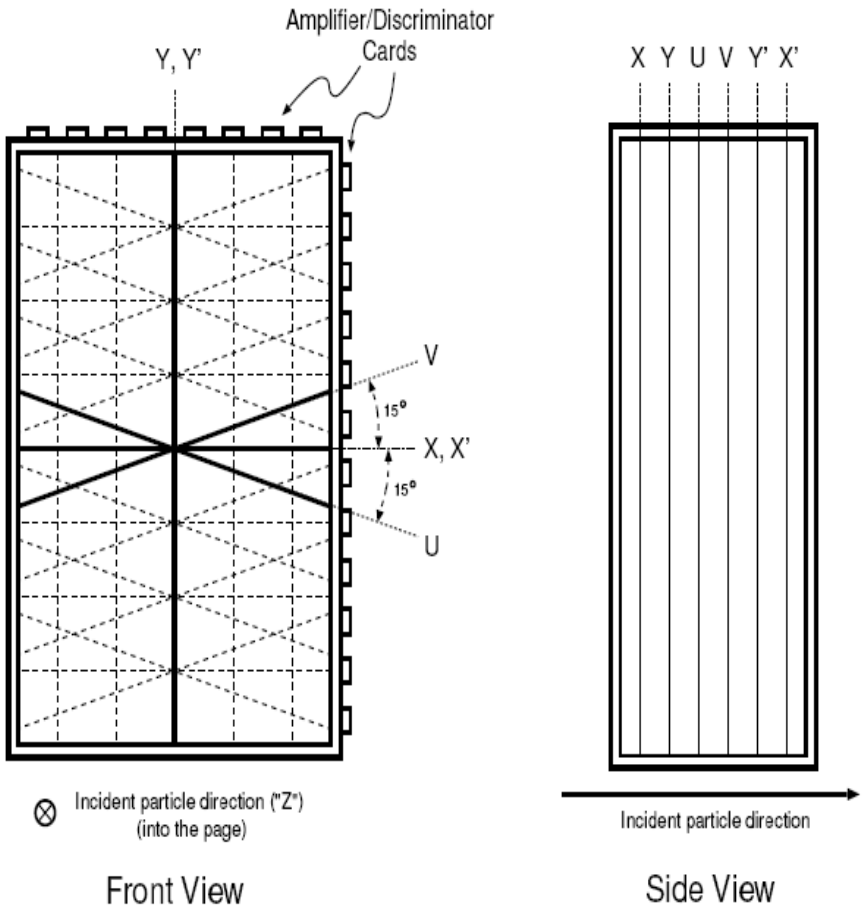

Coordinate resolution is about 300 μm.

Hodoscopes

Four hodoscopes for trigger.

Each paddle is 1 cm thick and 8 cm wide.

Hodoscopes are grouped in two horizontal-vertical (X-Y) pairs.

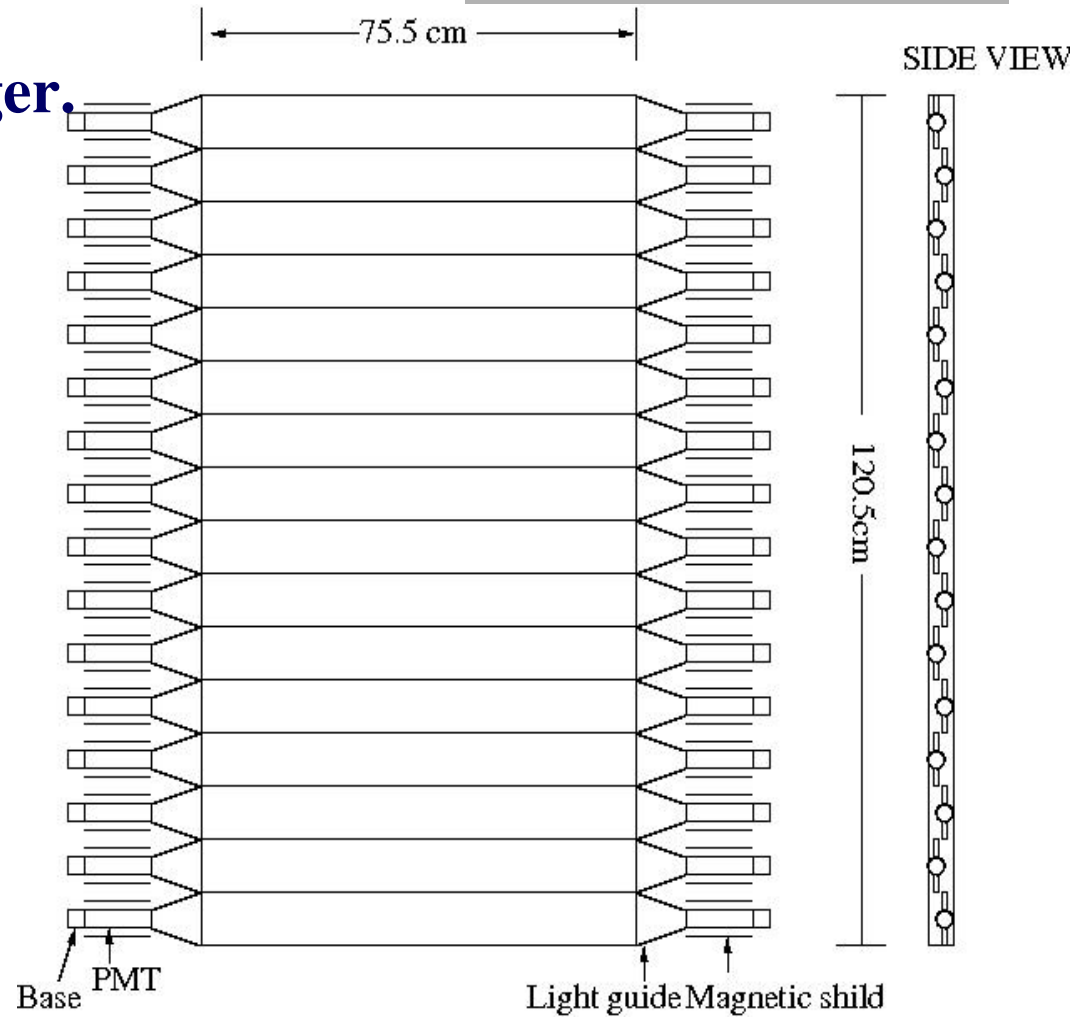

X hodoscopes have 16 horizontally placed scintillators.

Y hodoscopes have 10 vertically placed scintillators.

Gas Cerenkov

Gas Cerenkov is used for PID and trigger.

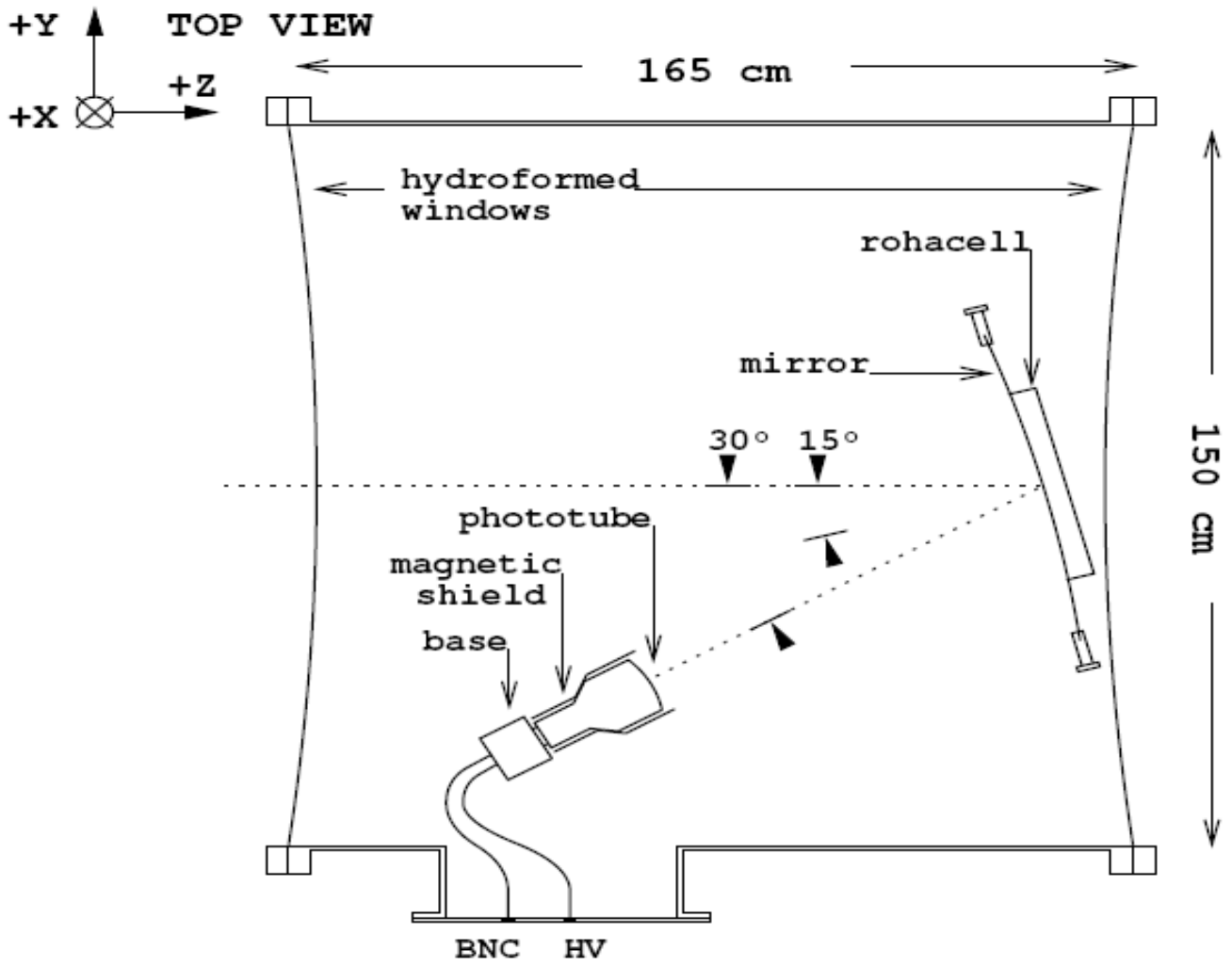

Gas Cerenkov

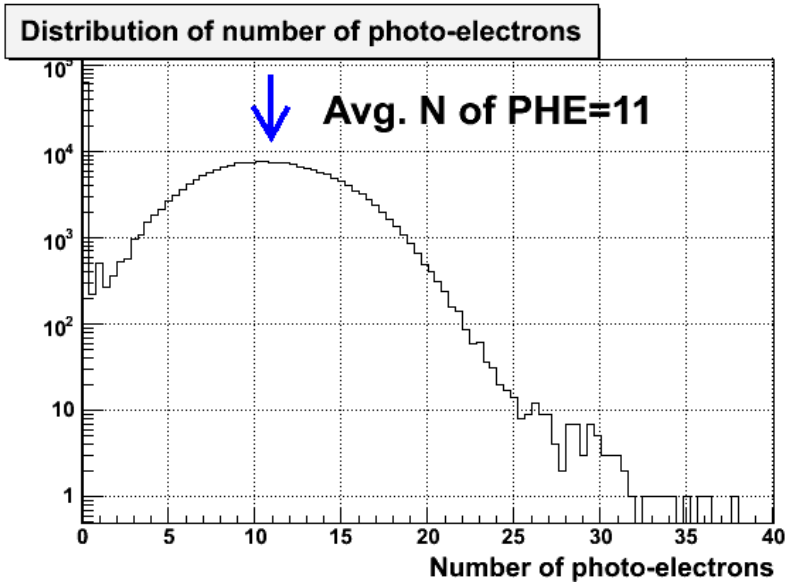

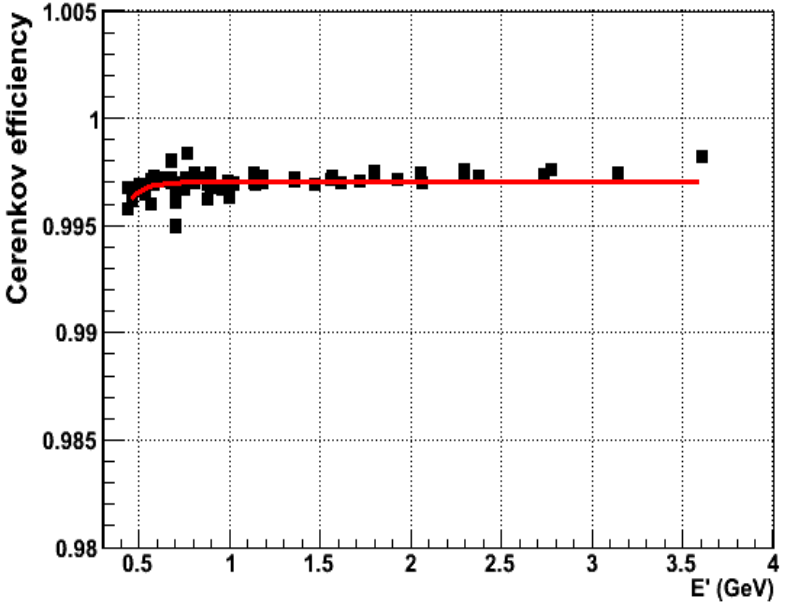

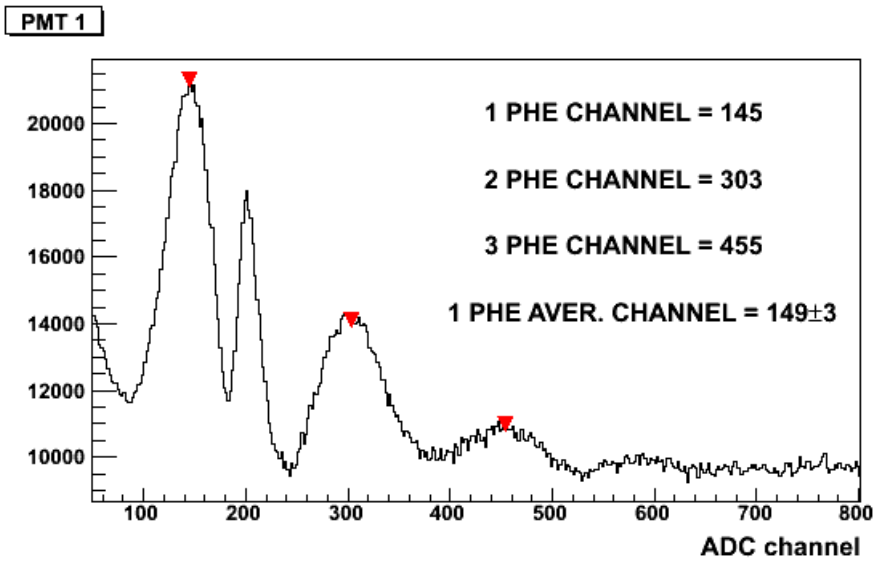

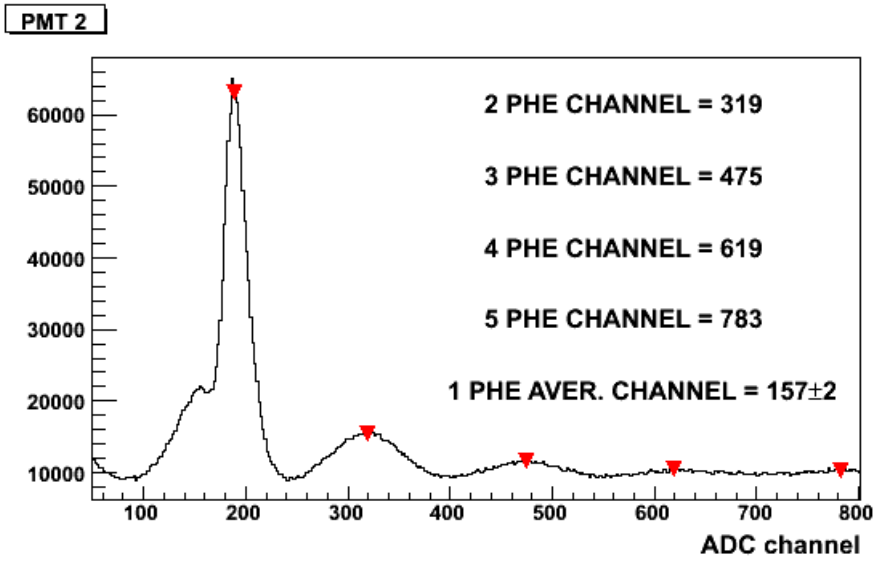

Calorimeter

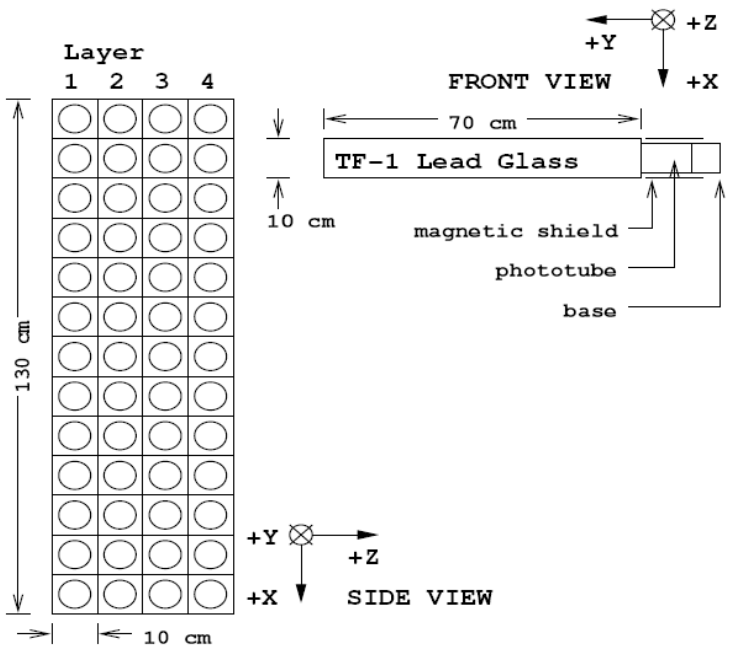

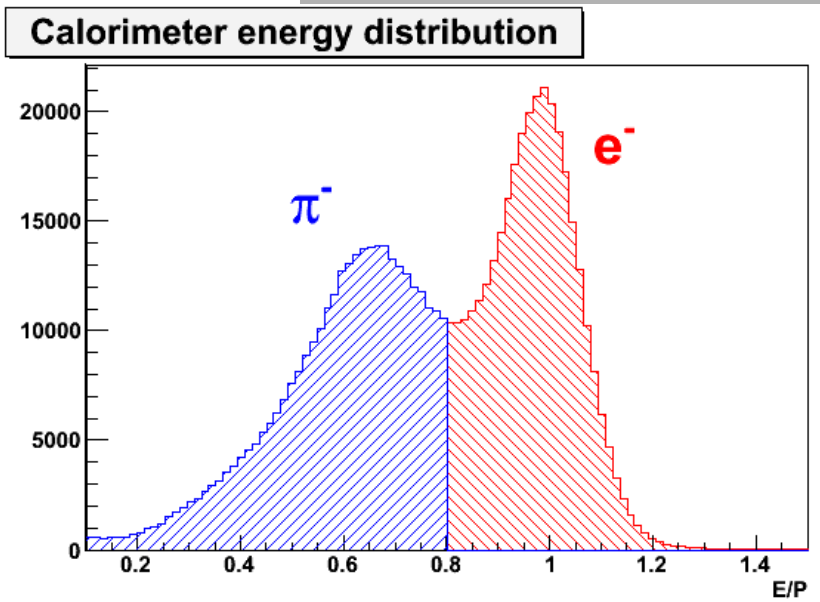

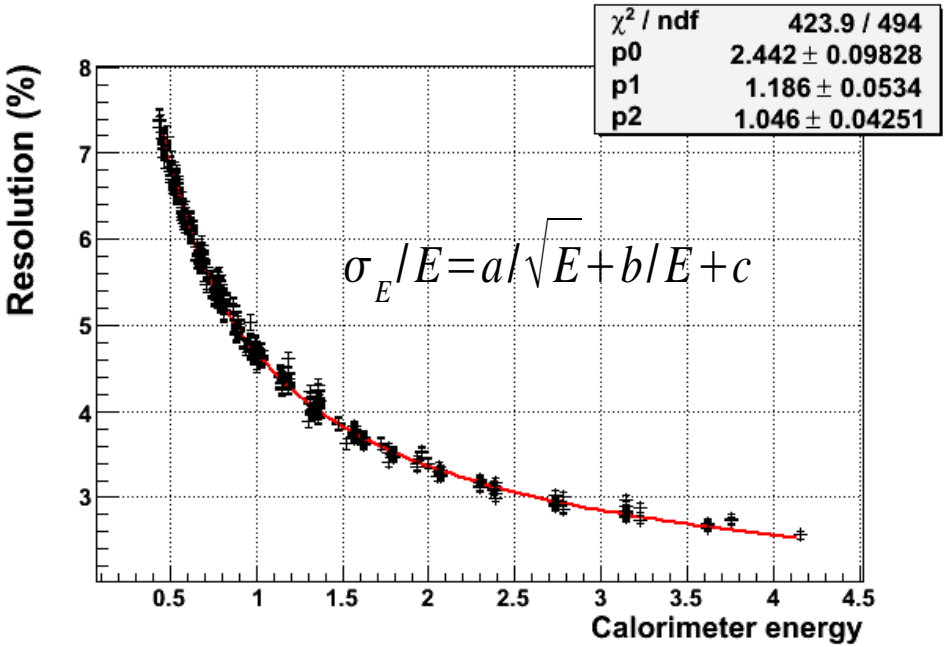

Calorimeter is used for trigger and particle identification.

Trigger

ELLO – requires Cerenkov signal and two out of

- ✔ At least one layer from S1 and S2
- ✔ At least 3 layers of S1 and S2
- ✔ Low energy signal from Calorimeter's first layer

ELHI – requires all

- ✔ High energy signal from Calorimeter's first layer
- ✔ At least 3 layers of S1 and S2
- ✔ Calorimeter energy above fixed threshold

ELREAL = ELLO OR ELHI

Trigger efficiency is very high thanks to using different combinations of Hodoscopes, Cerenkov and Calorimeter.

Trigger Efficiency

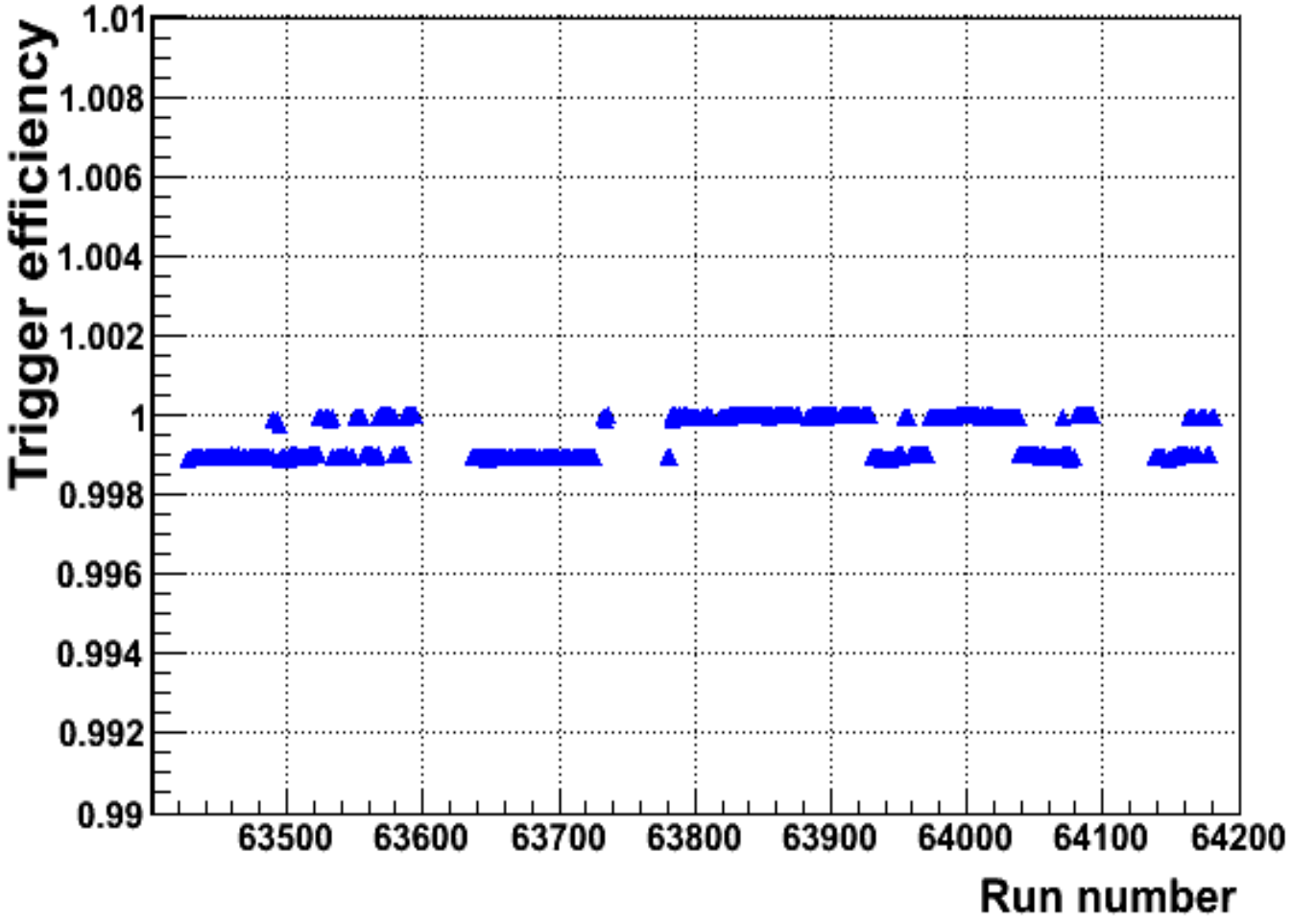

Kinematics Range

- Measurements for each energy are done at least for 3 different angles.
- Wide epsilon range allows Rosenbluth separation.

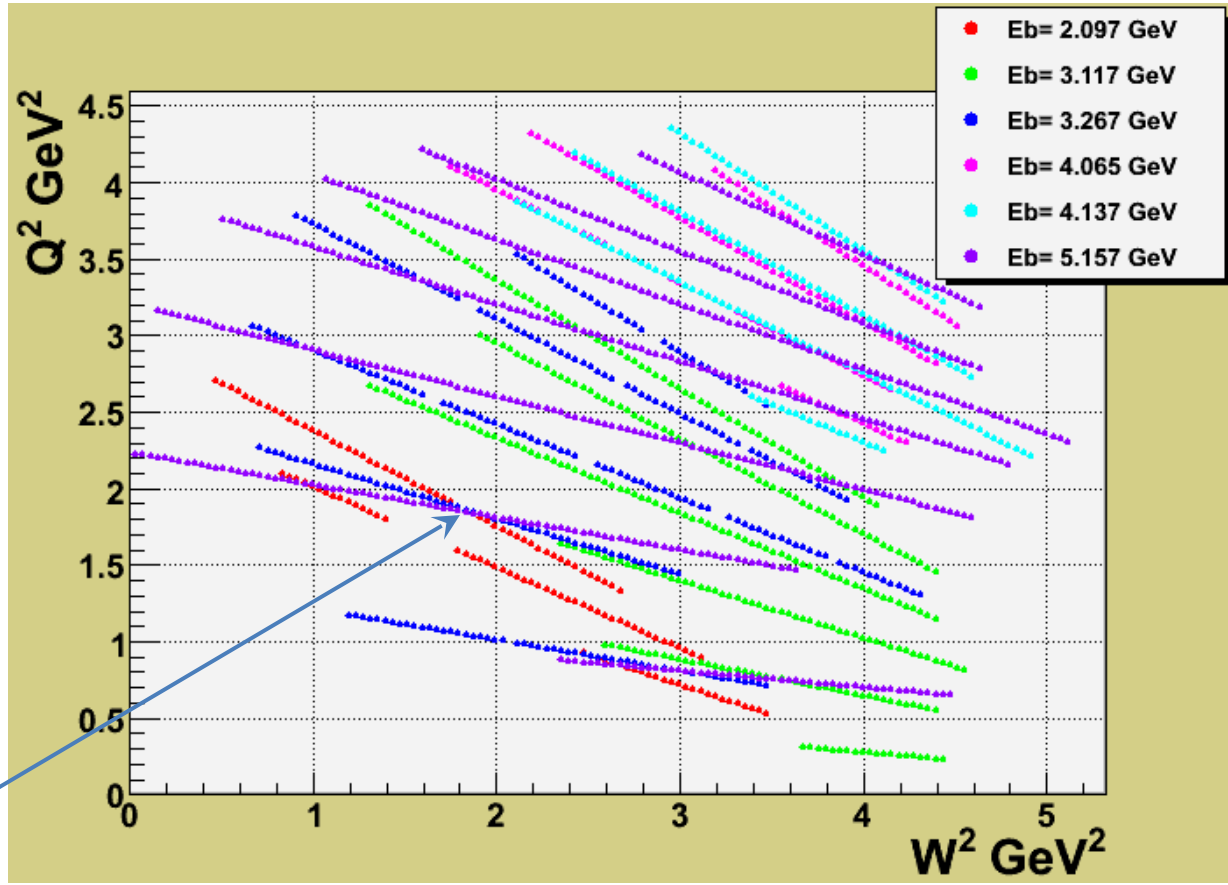

New data with $Q^2 > 3$ GeV^2

Targets : C, Al, Cu, Fe.

Different epsilon values for same Q^2 and W^2, allows LT separation.

New data compliments data from experiment E02-109.

Precision Cross Section Measurement

- ✓ **High statistic and good systematic precision.**
- ✓ **Wide range of counting rate, from a 1 kHz to 1 MHz. Keep trigger efficiency high for all rates.**
- ✓ **Linearity of detector response.**
- ✓ **Charge measurement by Beam Current Monitors.**
- ✓ **Corrections.**
  - **Background.**
  - **Acceptance.**
  - **Detector efficiency (Cerenkov, Calorimeter).**
  - **Tracking efficiency.**
  - **Radiative.**
  - **Bin centering.**

Events Selection and Backgrounds

- ✓ Gas Cherenkov detector for pion rejection.
- ✓ Electromagnetic calorimeter to increase pion rejection power at low energies.
- ✓ Combined pion rejection power of better then 100:1 for momentum range 0.4-4.2 GeV.

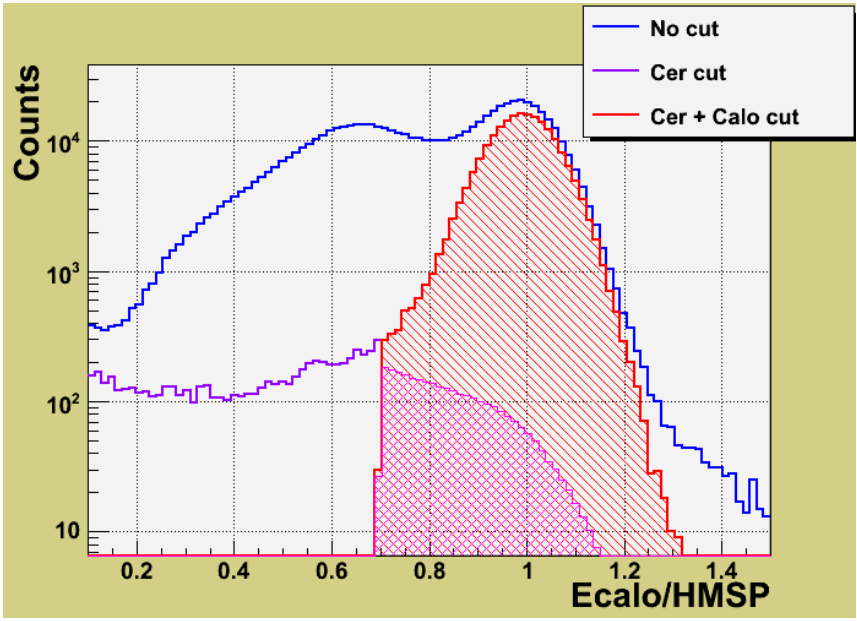

- ✓ Background e^- from π° and γ decay, Charge Symmetric Background (CSB) – Subtracting positrons for the same kinematics at positive HMS polarity.
- ✓ Negative pions π^- corrected after applying CSB.

Backgrounds - CSB

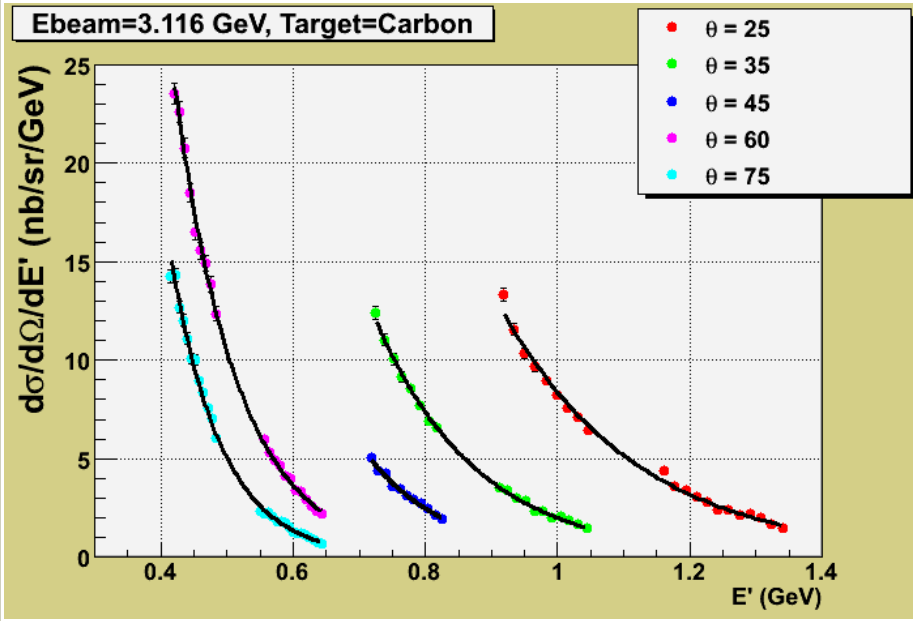

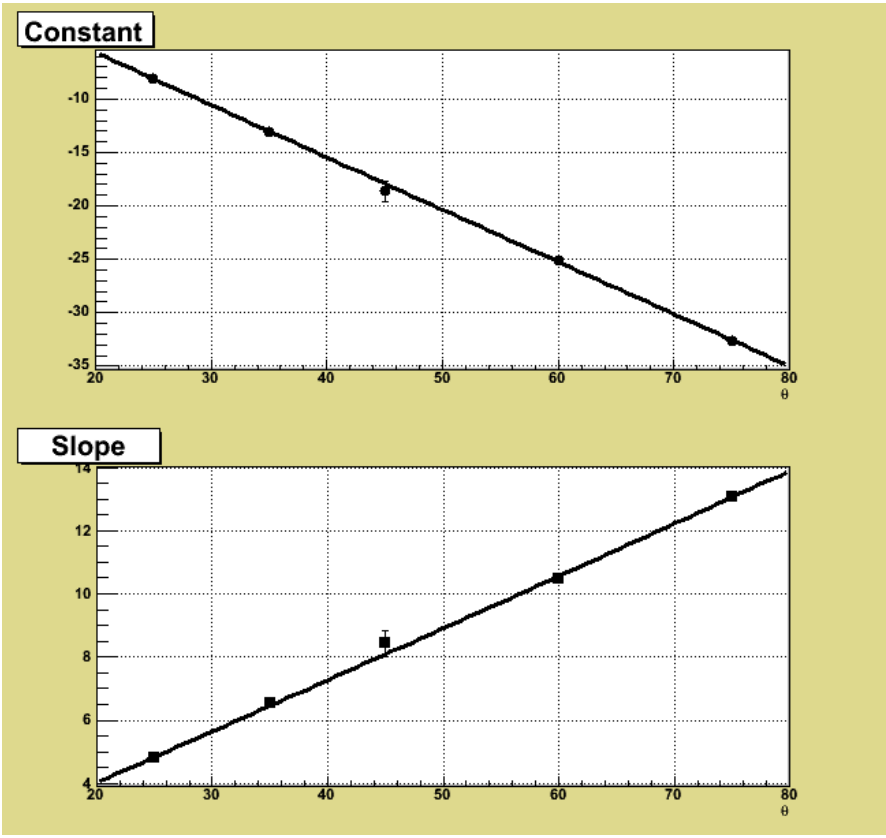

Cross Section(CS) fit function has exponential form, with constraint CS(E'=Ebeam,θ)=0.

$$\sigma(E',\theta = const) = \log(Const)\cdot(\exp(Slope\cdot(Ebeam - E')) - 1)$$

Cross section is interpolated by a polynomial in theta and used in CSB subtraction.

Cross Section Extraction

Cross section $\frac{d^2\sigma(\theta, E')}{d\Omega\, dE'} = \frac{Yield}{A(E', \theta) \times \Delta\Omega \times L \times EFF}$

Where:

- A(E´,θ): acceptance correction.
- L: integrated luminosity.
- Eff: total efficiency of detecting an electron.

A(E´,θ) acceptance correction is calculated from Monte Carlo.

Radiative and Bin Centering Corrections

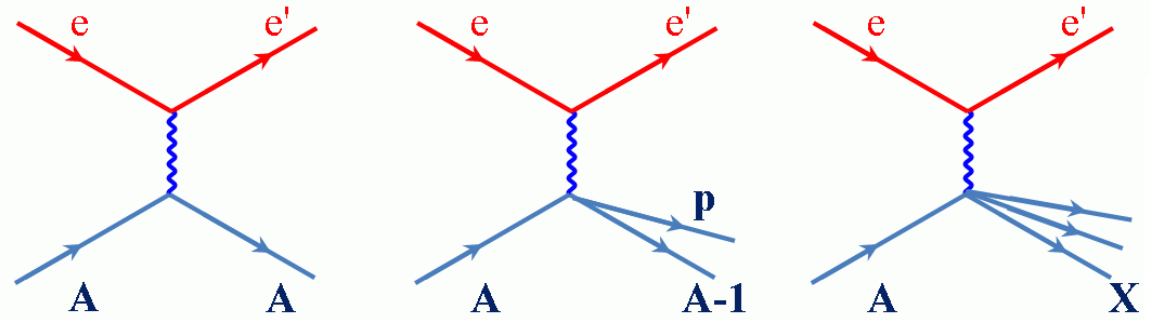

Elastic **Quasi-elastic** **Inelastic**

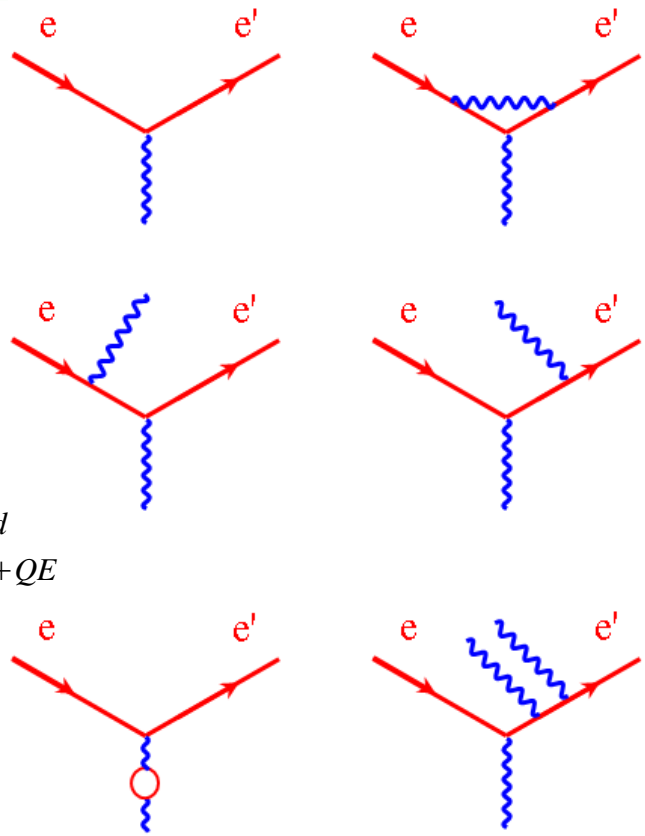

IE+ QE rad. corrected CS

$$\sigma^{\exp}_{IE+QE}(\theta, E') = (\sigma^{\exp}_{All} - \sigma^{mod}_{RadEl}) / (\sigma^{mod}_{RadAll} - \sigma^{mod}_{RadEl}) \times \sigma^{mod}_{IE+QE}$$

Bin correction factor

$$BC(\theta_i, E_j') = \sigma^{mod}_{RadAll}(\theta_o, E_j') / \sigma^{mod}_{RadAll}(\theta_i, E_j')$$

Bin centered CS, FINAL !

$$\sigma(\theta_o, E_j) = \frac{\sum_j^n \sigma(\theta_i, E_j) BC(\theta_i, E_j) / (\Delta\sigma(\theta_i, E_j) BC(\theta_i, E_j))^2}{\sum_j^n 1 / (\Delta\sigma(\theta_i, E_j) BC(\theta_i, E_j))^2}$$

Preliminary Results

Carbon

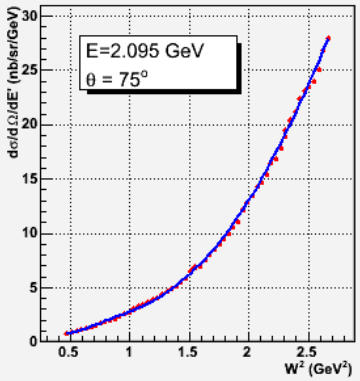

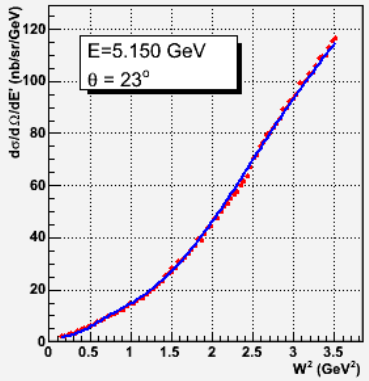

Iron

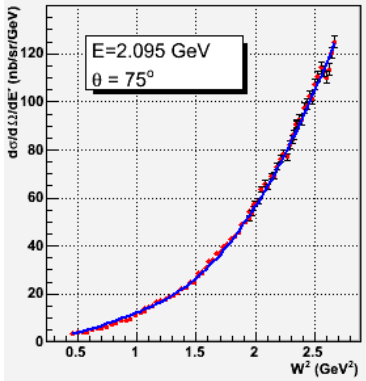

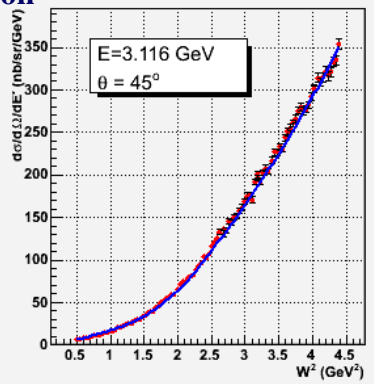

Aluminum

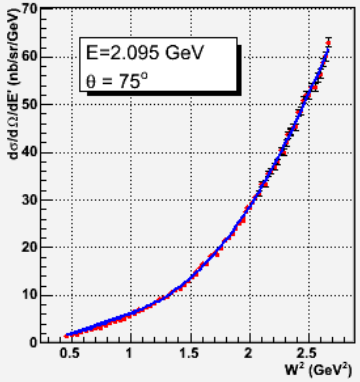

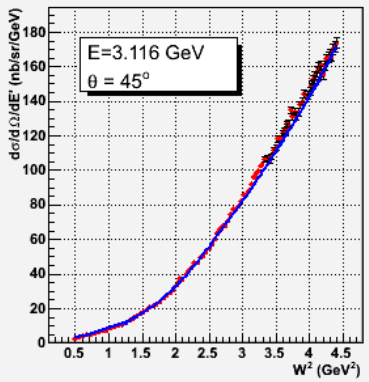

Copper

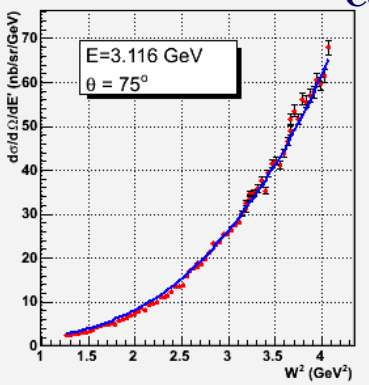

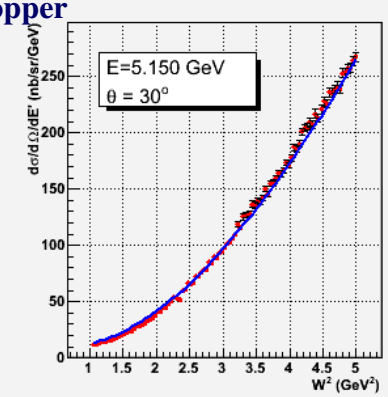

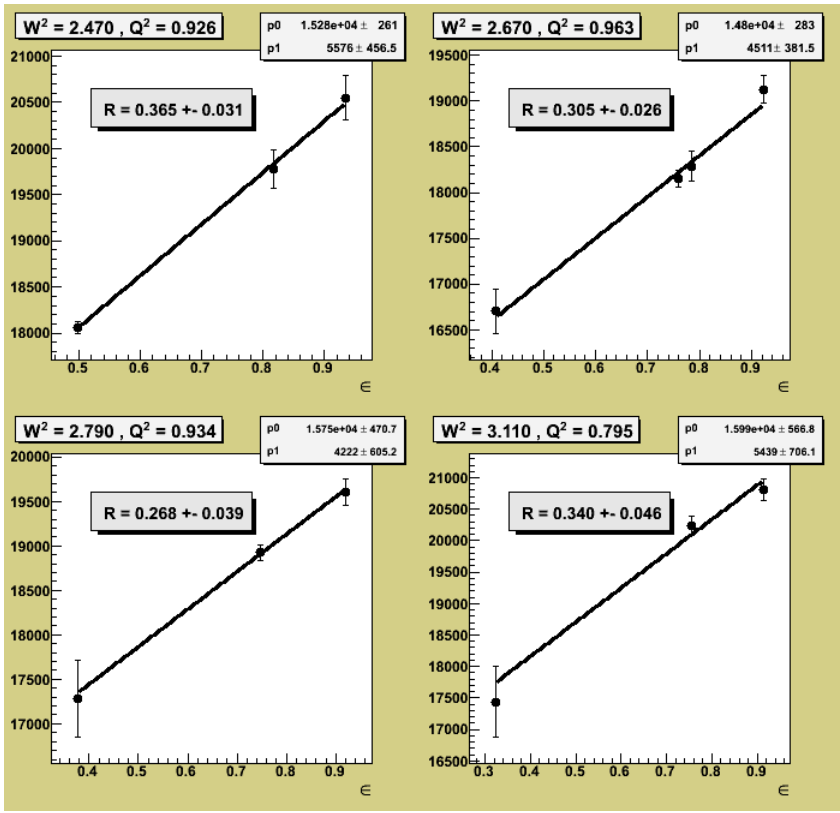

Cross Section Ratios σ_A/σ_D

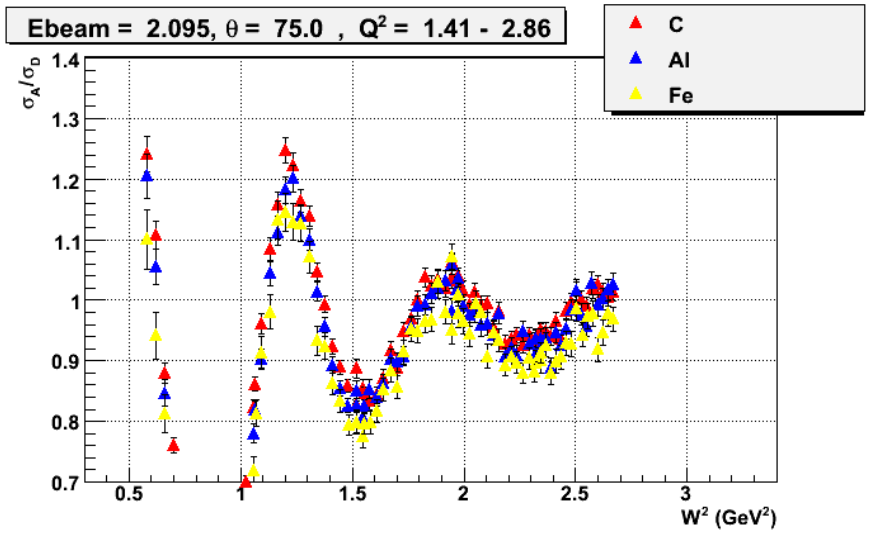

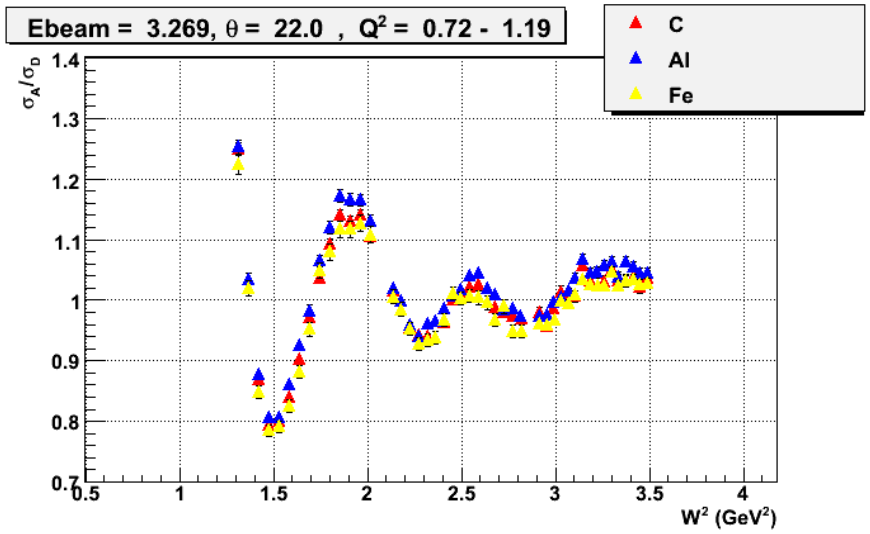

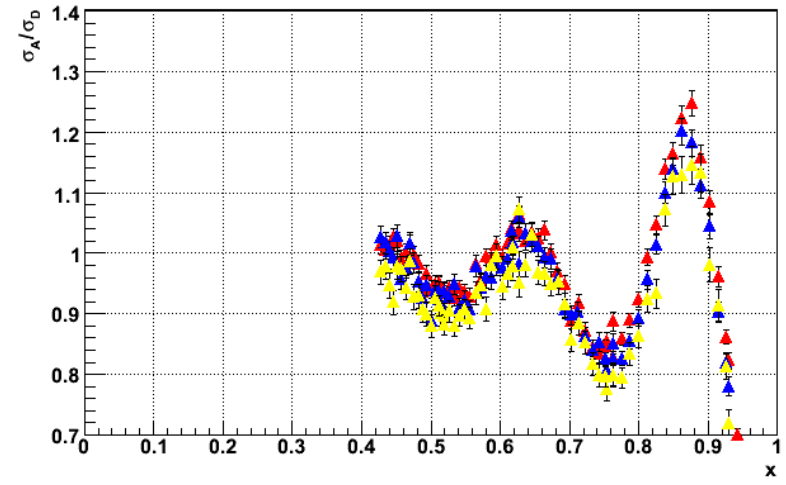

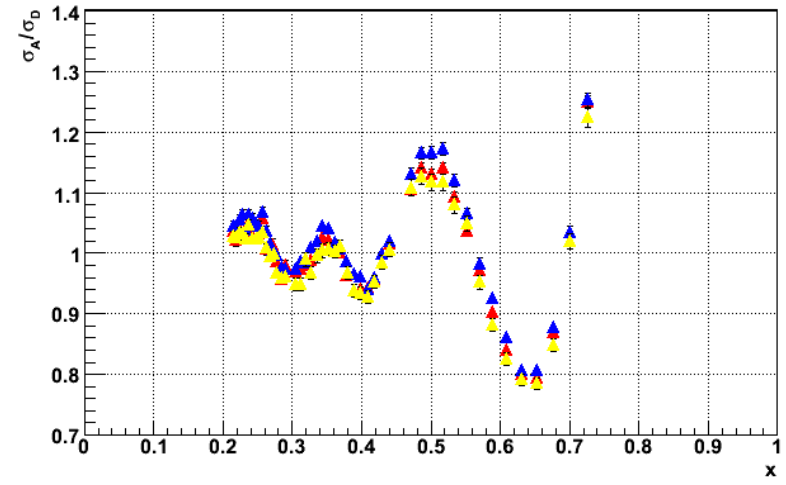

Global Fit and Iteration Procedure

Model cross section for nucleus is based on the empirical fit of proton and deuterium.

F_1, F_2 inelastic are based on:

- ✔ **Empirical Fit to Precision Inclusive Electron-Proton Cross Sections in the Resonance Region hep-ph/0712.3731.**

- ✔ **Empirical Fit to Inelastic Electron-Deuteron and Electron-Neutron Resonance Region Transverse Cross Sections hep-ph/0711.0159.**

F_1, F_2 quasi-elastic are based on:

- ✔ **Super scaling from Sick, Donnelly, Mairon nucl-th/0109032.**

Global Fit – Structure Functions

Isoscalarity correction, takes into account the excess of neutrons

$$W_1^A = \frac{(2Z F_1^D + (A-2Z)(2F_1^D - F_1^P))}{M_P}$$

Meson Exchange Current, pure empirical form to improve the fit.

$$W_1^{A,Corr} = W_1^A + W_1^{MEC}$$

Where MEC term is added to improve the fit. The functional form does not any physical meaning.

It is assumed that R is the same for proton and neutron.

R_D is evaluated by Fermi smearing.

$$W_2^A = W_1^{A,Corr}(1+R_D)/(1+\nu^2/Q^2)$$

Global Fit – EMC effect

Nuclear structure functions are different from structure functions of nuclei.

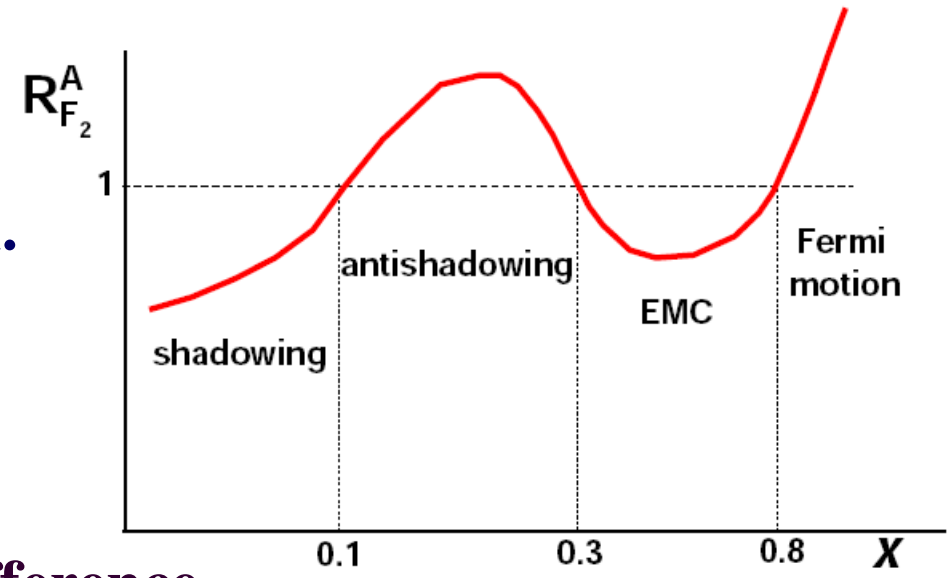

$$R_{F_2}^A(x,Q^2)=\frac{F_2^A(x,Q^2)}{AF_2^{nucleon}(x,Q^2)}$$

In our fit we correct that difference.

For x>0.125 SLAC-E139 fit was used.

For x<0.0085-0.09 Amaudruz et al Z. Phys C. 51,387(91).

$$F_1^A=M_P W_1^A EMCCORR(x,A) \qquad F_2^A=\nu W_2^A EMCCORR(x,A)$$

$$\frac{d^2\sigma}{d\Omega\, dE'}=\frac{4\alpha^2(E')^2}{Q^4}\left[\cos^2\frac{\theta}{2}W_2(\nu,q^2)+2W_1(\nu,q^2)\sin^2\frac{\theta}{2}\right]$$

Global Fit - Results

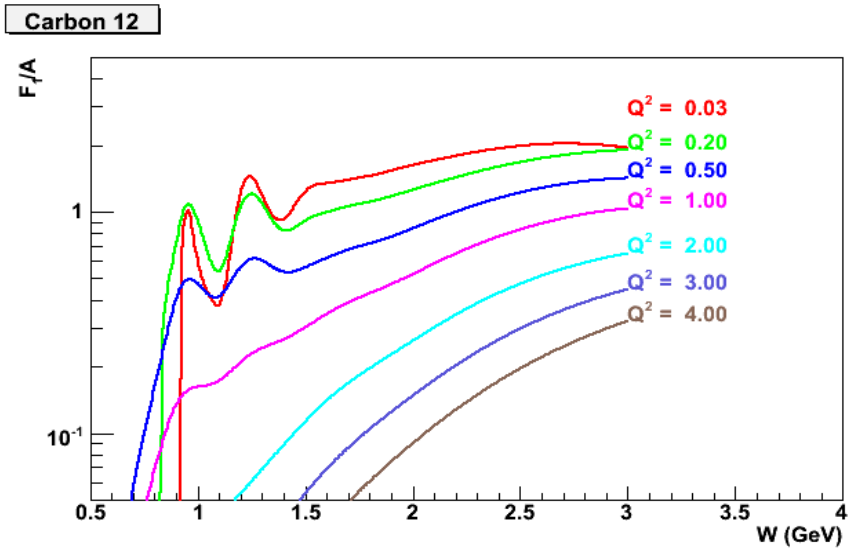

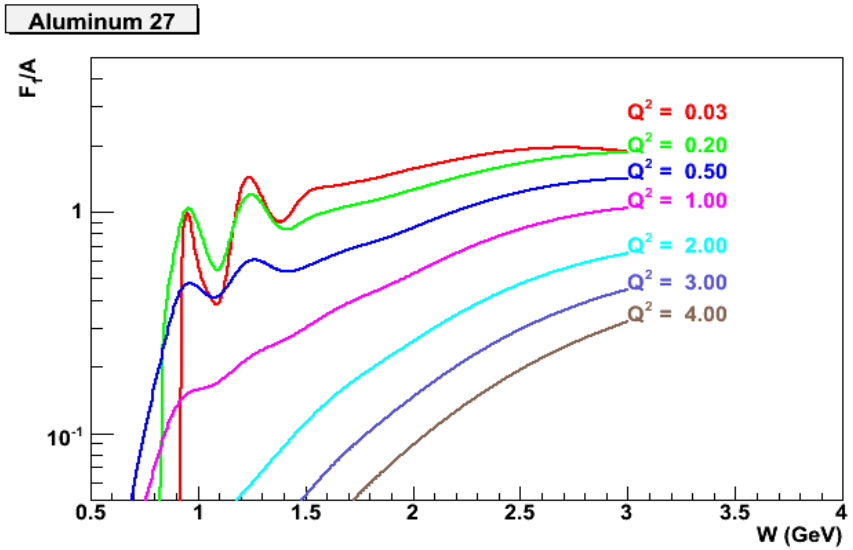

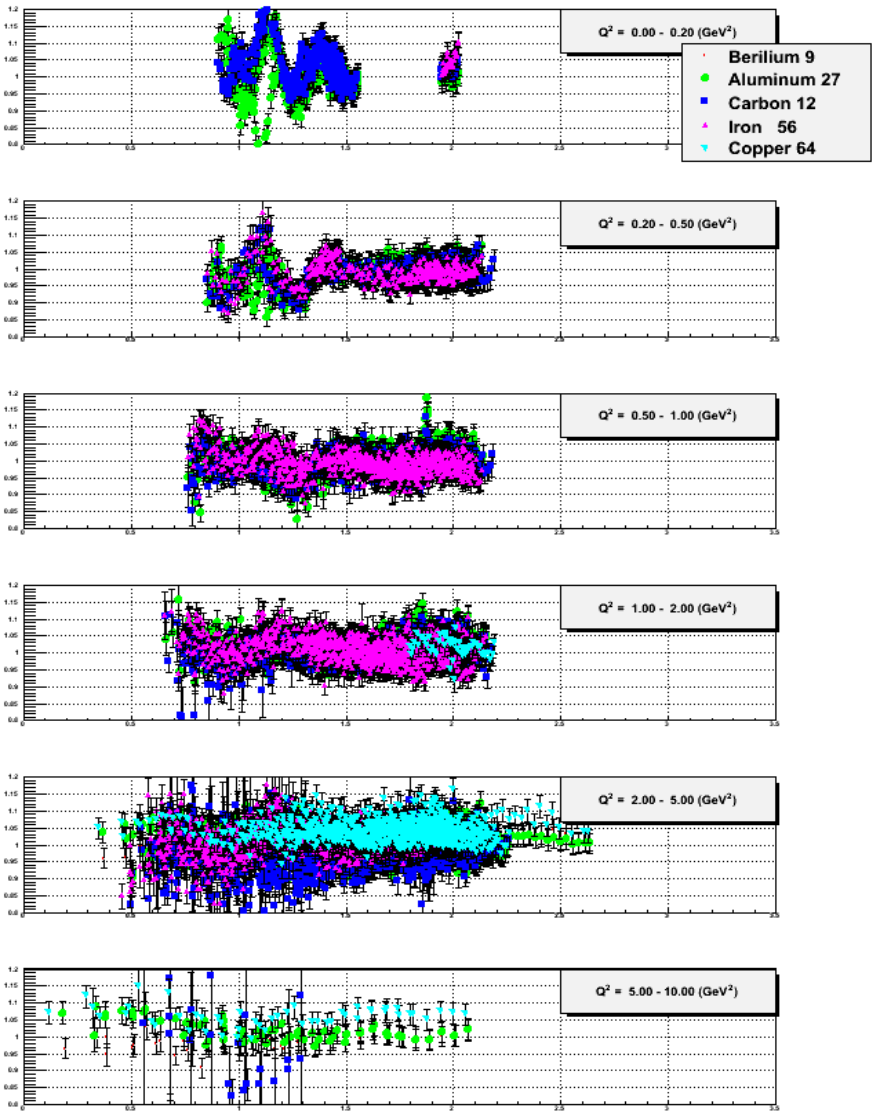

Global Fit - Results

Frequency distribution for the deviations from unity of the ratios of data to fit.

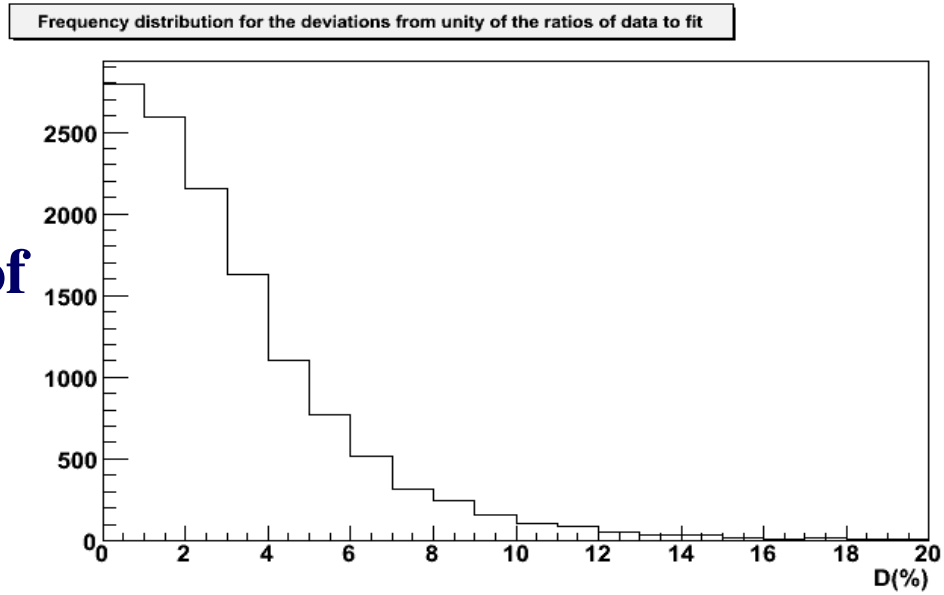

Percentage of points which agree with the fit within given deviation from unity.

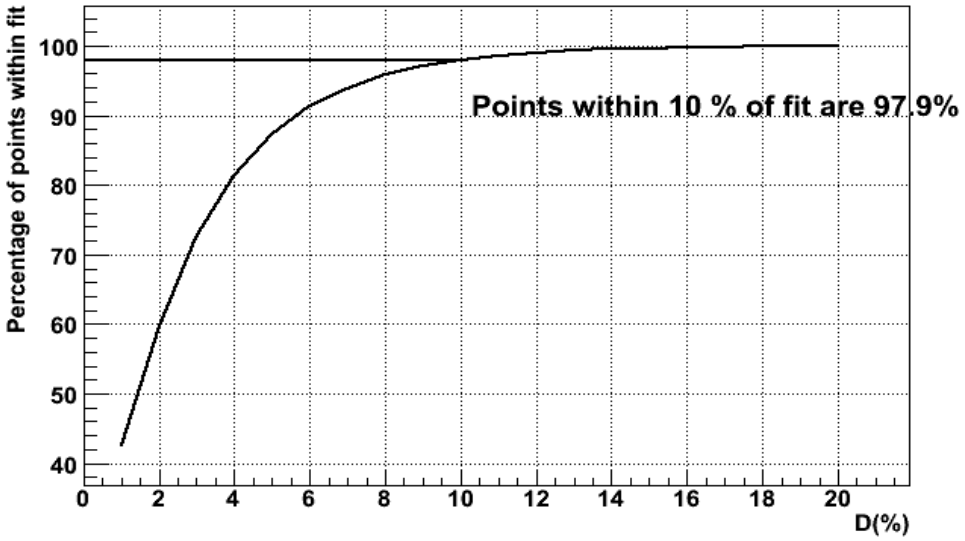

Summary

- ✓ **JLab's Hall C allows high precision measurements of nuclear structure functions by performing Rosenbluth separation.**
- ✓ **New data in Nuclear Resonance region enhances our knowledge of nuclear structure.**
- ✓ **Quark-hadron duality gives an opportunity to study possible link between confinement and asymptotic freedom.**
- ✓ **Measurements of nuclear structure functions F_L, F_1, F_2 allow the study of electromagnetic and weak structure.**
- ✓ **Reduction of uncertainties of neutrino oscillation parameters in future neutrino oscillation experiments.**

Appendix

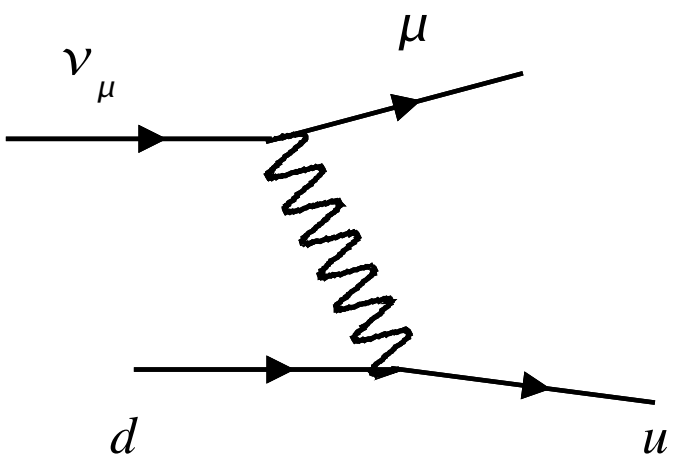

$$\nu_\mu d \to u \mu^- \qquad \bar{\nu}_\mu \bar{d} \to \bar{u} \mu^+$$

$$\nu_\mu s \to u \mu^- \qquad \bar{\nu}_\mu \bar{s} \to \bar{u} \mu^+$$

$$\nu_\mu \bar{u} \to \bar{d} \mu^- \qquad \bar{\nu}_\mu u \to d \mu^+$$

$$\nu_\mu \bar{u} \to \bar{s} \mu^- \qquad \bar{\nu}_\mu u \to s \mu^+$$